Carbon quantum dots anchored on 1,2,3,5-tetrakis(carbazole-9-yl)-4,6-dicyanobenzene for efficient selective photo splitting of biomass-derived sugars to lactic acid

Xiaopan Yang, [a] Kangning Liu, [a] Jiliang Ma, [a,b,c*] Runcang Sun [a *]

[a] Liaoning Key Lab of Lignocellulose Chemistry and Biomaterials, Liaoning Collaborative Innovation Center for Lignocellulosic Biorefinery, College of Light Industry and Chemical Engineering, Dalian Polytechnic University, Dalian, China, 116034

[b] Guangxi Key Laboratory of Clean Pulp & Papermaking and Pollution Control, College of Light Industrial and Food Engineering, Guangxi University, Nanning, 530004

[c] National Forestry and Grassland Administration Key Laboratory of Plant Fiber Functional Materials, Fuzhou, Fujian, China, 350108

*Corresponding authors' E-mail: jlma@dlpu.edu.cn (Jiliang Ma), and rcsun3@dlpu.edu.cn (Runcang Sun), Tel.: +86-0411-86323652; Fax: +86-0411-86323652.

1. Experimental section

1.1 Materials

For all chemicals and solvents were analytical grade. Xylose ($C_5H_{10}O_5$, ≥ 99%)，fructose ($C_6H_{12}O_6$, ≥ 99%)， glucose ($C_6H_{12}O_6$, 96%)， mannose ($C_6H_{12}O_6$, 99%), arabinose ($C_5H_{10}O_5$, 98%), rhamnose ($C_6H_{12}O_5 \cdot H_2O$, 99%), benzoquinone (BQ), potassium iodide (KI), isopropyl (IPA) and tryptophan (Trp) were all purchased from Aladdin Chemistry Co., Ltd (Shanghai, China). 1,2,3,5-tetrakis(carbazole-9-yl)-4,6-dicyanobenzene (4CzIPN, 98.0%) was purchased from Wohler Organic. Ethylenediamine and citric acid were purchased from China National Pharmaceutical Chemical Reagent Co. Anhydrous ethanol was purchased from Tianjin Kermio Chemical Reagent Co., Ltd (Tianjin, China).

1.2 Characterization

Transmission electron microscopy (TEM) were recorded on JEM-2100 CXII and scanning electron microscopy (SEM) were explored on Hitachis-4800. Fourier infrared (FT-IR) spectrum were taken on a Bruker Tensor 27 spectrophotometer in the range of 400-4000 cm^{-1} with a resolution of 4 cm^{-1}. The powder X-ray diffraction (XRD) patterns were measured with a Bruker D8 Focus diffractometer (CuKα radiation, λ = 0.15418 nm) in the θ-2θ mode. Brunauer-Emmett-Teller (BET) specific surface areas were measured on a Micromeritics ASAP 2020 apparatus. The X-ray photoelectron spectroscopy (XPS) analysis was performed with a Kratos Axis Ultra DLD spectrometer employing an amonochromated AlKR X-ray source (1486.6 eV). The ultraviolet-visible diffuse reflectance spectrum (UV-vis DRS) was achieved on a Cary 5000 spectrophotometer by using $BaSO_4$ as the reference. The photoluminescence (PL) spectrum was measured by an Edinburgh FLS-920 spectrometer. Electron spin-resonance spectroscopy was used to study molecules and materials with unpaired electrons, and the 5,5-dimethyl-1-pyrroline N-oxide (DMPO) was chosen as a spin trap for the detection of hydroxyl radical (·OH) and superoxide ($\cdot O_2^-$), the 2,2,6,6-tetramethylpiperidine-1-oxyl (TEMPO) was applied to characterize electrons and holes, while the amino-2,2,6,6-tetramethylpiperidine (TEMPONE) was used to detect singlet oxygen. Ultraviolet photoelectron spectroscopy (UPS) was measured by using a He I (21.20 eV) as monochromatic discharge light source and a VG Scienta R4000 analyzer. A sample bias of -5 V was applied to observe the secondary electron cutoff (SEC).

2. Results and discussion

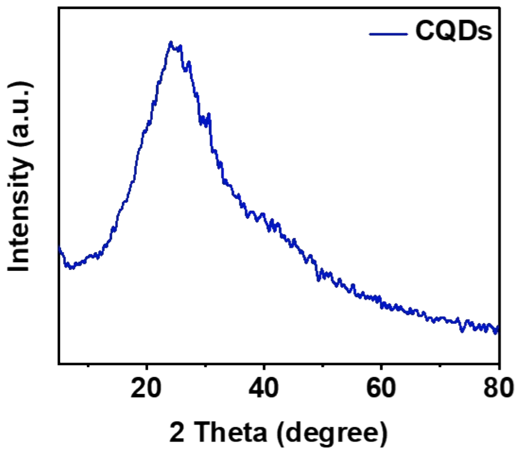

Fig. S1. XRD patterns of CQDs.

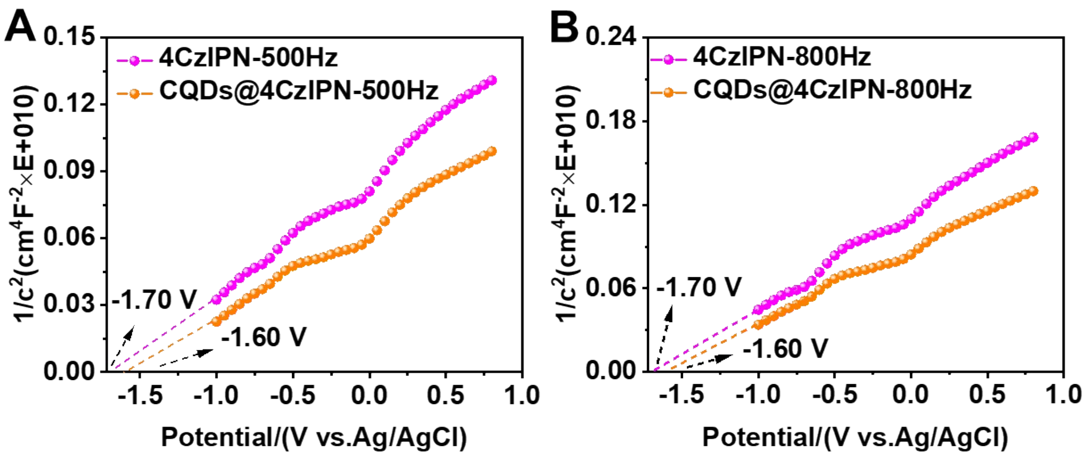

Fig. S2. Mott-Schottky plots of 4CzIPN and CQDs@4CzIPN at frequencies of 500 Hz (A) and 800 Hz (B) in 0.5 M Na_2SO_4.

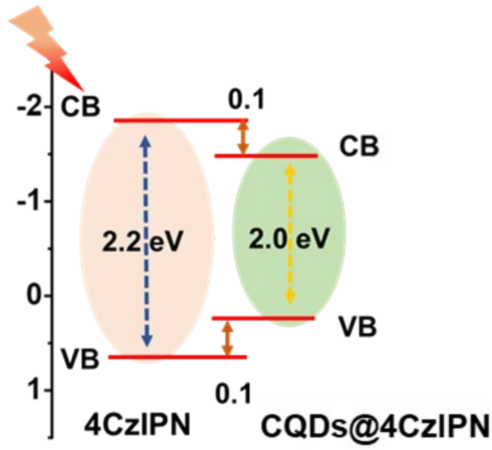

Fig. S3. Relative band alignment of 4CzIPN and CQDs@4CzIPN.

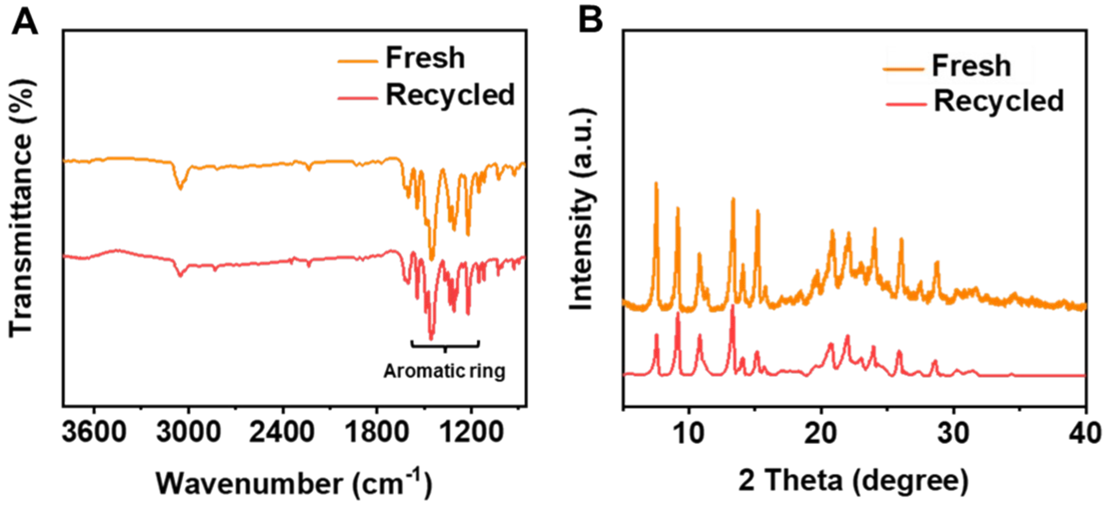

Fig. S4. FT-IR spectra (A) and XRD patterns (B) of the fresh and recycled CQDs@4CzIPN.

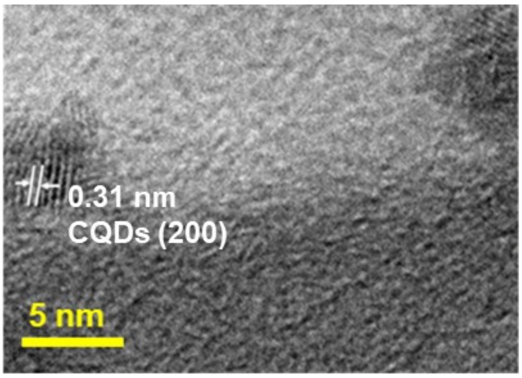

Fig. S5. The HRTEM image of the recycled CQDs@4CzIPN.

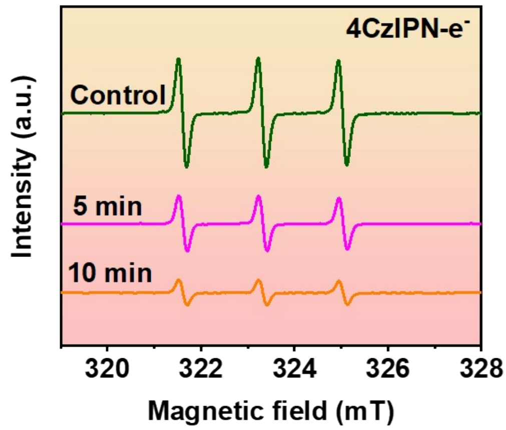

Fig. S6. TEMPO ESR spin-labeling for e⁻.

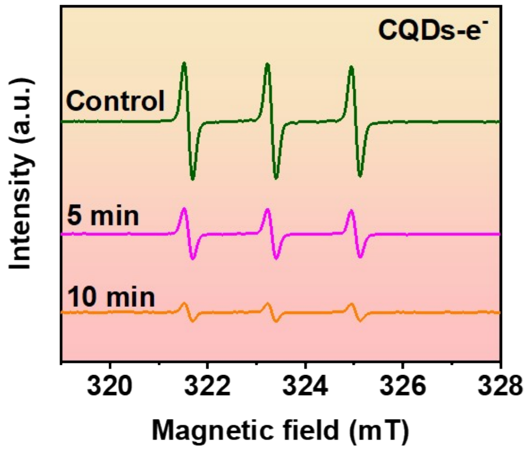

Fig. S7. TEMPO ESR spin-labeling for e^-.

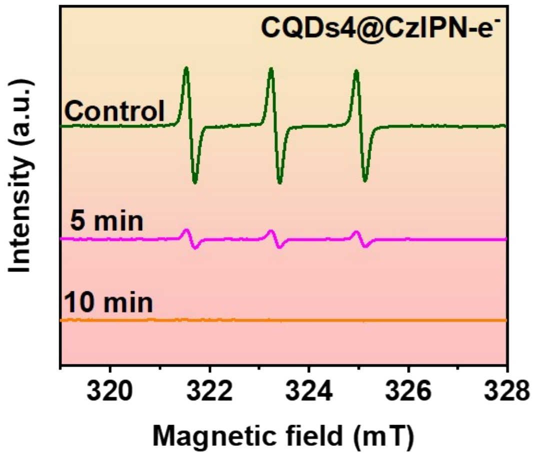

Fig. S8. TEMPO ESR spin-labeling for e^-.

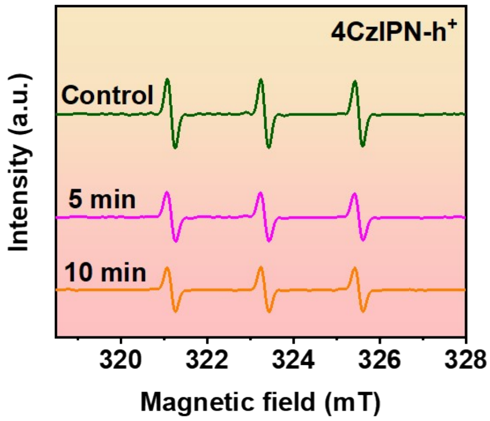

Fig. S9. TEMPO ESR spin-labeling for h^+.

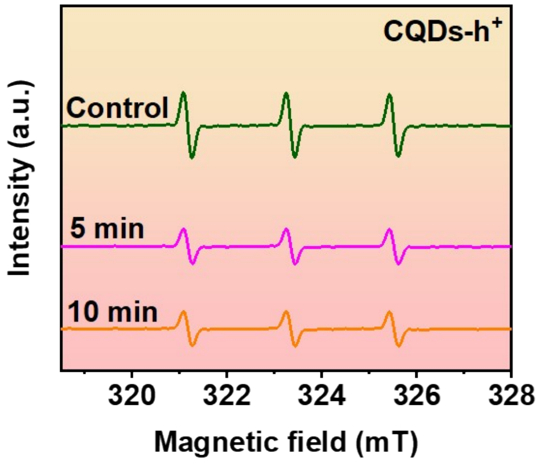

Fig. S10. TEMPO ESR spin-labeling for h^+.

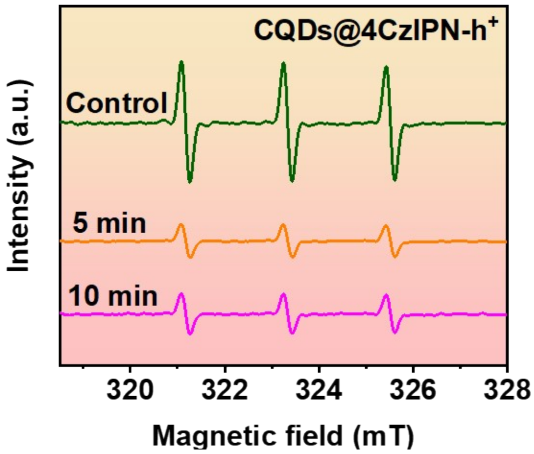

Fig. S11. TEMPO ESR spin-labeling for h^+.

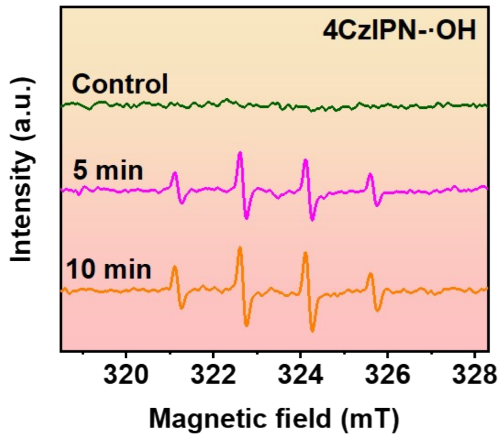

Fig. S12. DMPO ESR spin-labeling for ·OH.

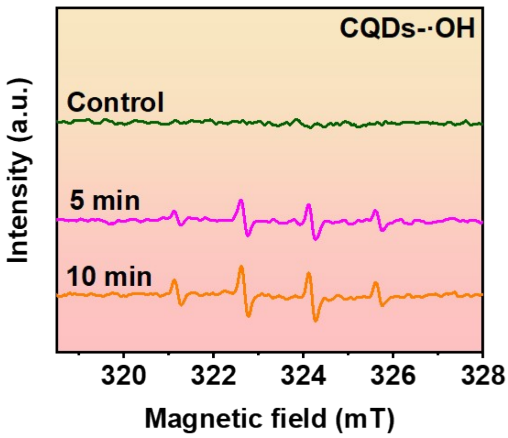

Fig. S13. DMPO ESR spin-labeling for ·OH.

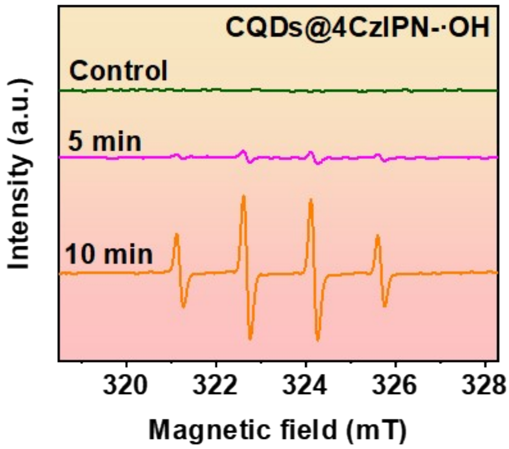

Fig. S14. DMPO ESR spin-labeling for ·OH.

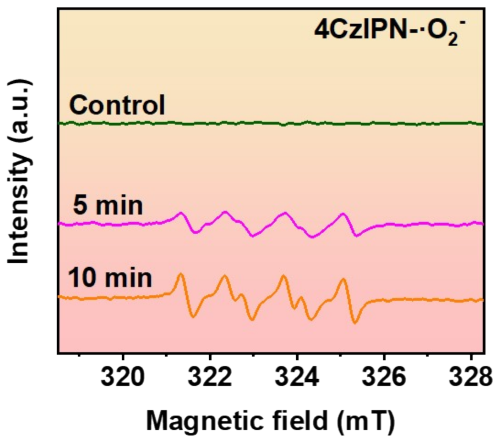

Fig. S15. DMPO ESR spin-labeling for $\cdot O_2^-$.

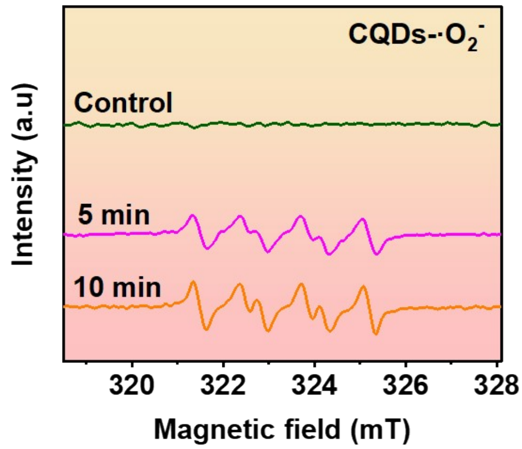

Fig. S16. DMPO ESR spin-labeling for $\cdot O_2^-$.

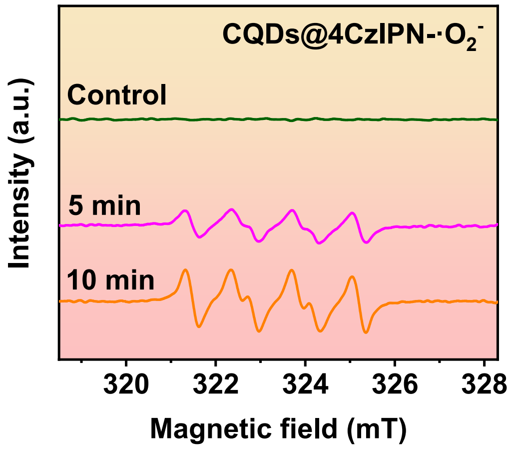

Fig. S17. DMPO ESR spin-labeling for $\cdot O_2^-$.

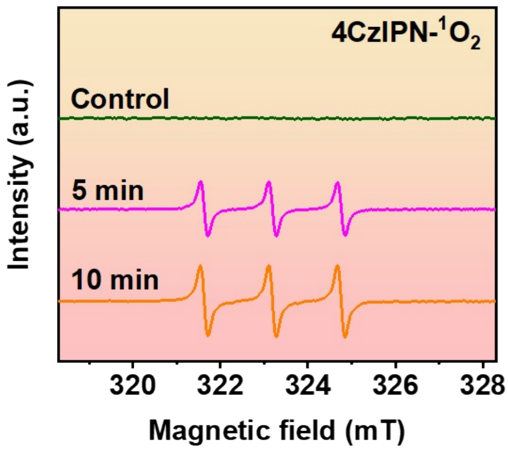

Fig. S18. TEMPONE ESR spin-labeling for $^1O_2$.

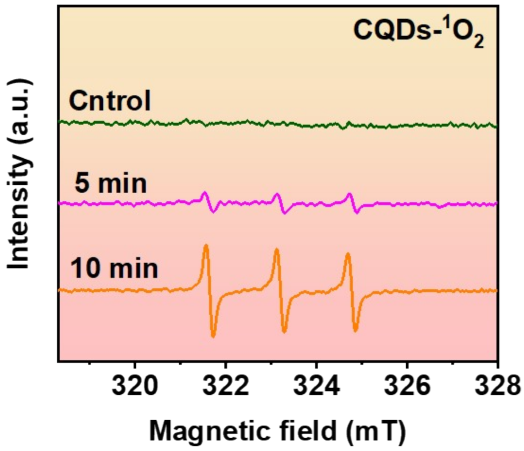

Fig. S19. TEMPONE ESR spin-labeling for $^1O_2$.

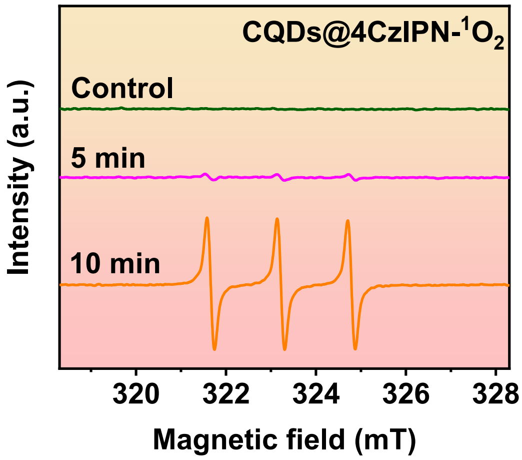

Fig. S20. TEMPONE ESR spin-labeling for $^1O_2$.

Table S1. The effects of different catalysts on the synthesis of lactic acid from different biomass-based monosaccharides with various conditions.

Entry	Samples	Thermo-catalysis	Photocatalysis	Conversion (%)	Yield (%)	Refs.
1	Xylose		CQDs@4CzIPN[a]	＞99.0	92.7	This work
2		Al-RT[b]		＞99.0	63.0	[1]
3		UiO-66[c]		＞98.3	70.2	[2]
4		SnBeta[d]		＞99.0	70.0	[3]
5			*Ut*-OCN[e]	＞99.0	89.7	[4]
6			B@*m*CN[f]	＞99.0	79.1	[5]
7	Fructose		CQDs@4CzIPN[a]	＞99.0	76.4	This work
8			*Ut*-OCN[e]	≥98.0	69.6	[4]
9		$(C_4H_9)_2SnO$[g]		＞99.0	63.0	[6]

Reaction condition: [a] 70.0 ^oC, 30.0 min. [b] 170.0 ^oC, N_2: 15.0 bar ,4.0 h. [c] 170.0 ^oC, N_2: 15.0 bar ,4.0 h. [d] 200.0 ^oC, N_2: 4.0 Mpa, 1 h. [e] 50.0 ^oC, 1.5 h. [f] 60.0 ^oC,90.0 min. [g] 210.0 ^oC, 30.0 min.

References

1 S. Kiatphuengporn, A. Junkaew, C. Luadthong, S. Thongratkaew, C. Yimsukanan, S. Songtawee, T. Butburee, P. Khemthong, S. Namuangruk and M. Kunaseth, Green Chem., 2020, **22**, 8572-8583.

2 P. Ponchai, K. Adpakpang, S. Thongratkaew, K. Chaipojjana, S. Wannapaiboon, S. Siwaipram, K. Faungnawakij and S. Bureekaew, *Chem. Commun.*, 2020, **56**, 8019-8022.

3 Y. F. Zhang, H. Luo, L. Z. Kong, X. P. Zhao, G. Miao, L. J. Zhu, S. G. Li and Y. H. Sun, *Green Chem.*, 2020, **22**, 7333-7336.

4 J. L. Ma, D. N. Jin, Y. C. Li, D. Q. Xiao, G. J. Jiao, Q. Liu, Y. Z. Guo, L. P. Xiao, X. H. Chen and X. Z. Li, *Appl. Catal. B-Environ.*, 2021, **283**, 119520.

5 J. L. Ma, Y. C. Li, D. N. Jin, Z. Ali, G. J. Jiao, J. Q. Zhang, S. Wang and R. C. Sun, *Green Chem.*, 2020, **22**, 6384-6392.

6 J. B. Dos Santos, N. J. A. de Albuquerque, C. L. D. P. E Silva, M. R. Meneghetti and S. M. P. Meneghetti, *RSC Adv.*, 2015, **5**, 90952-90959.